

# Highly-Efficient Gating of Solid-State Nanochannels by DNA Supersandwich Structure Containing ATP Aptamers: A Nanofluidic IMPLICATION Logic Device

Yanan Jiang,<sup>§,⊥</sup> Nannan Liu,<sup>‡,⊥</sup> Wei Guo,<sup>\*,†</sup> Fan Xia,<sup>\*,‡</sup> and Lei Jiang<sup>†,§</sup>

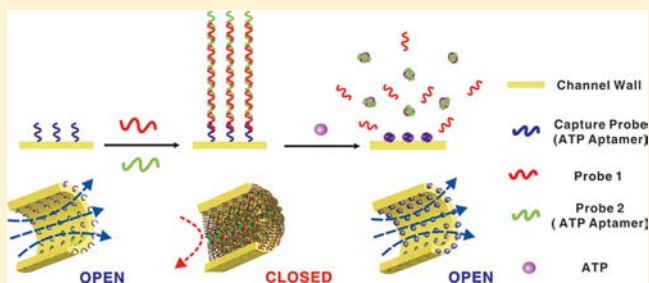
<sup>†</sup>Beijing National Laboratory for Molecular Sciences (BNLMS), Key Laboratory of Organic Solids, Institute of Chemistry, Chinese Academy of Sciences, Beijing 100190, P.R. China

<sup>‡</sup>School of Chemistry and Chemical Engineering, Huazhong University of Science and Technology, Wuhan 430074, P.R. China

<sup>§</sup>School of Chemistry and Environment, Beijing University of Aeronautics and Astronautics, Beijing 100191, P.R. China

## Supporting Information

**ABSTRACT:** Integrating biological components into artificial devices establishes an interface to understand and imitate the superior functionalities of the living systems. One challenge in developing biohybrid nanosystems mimicking the gating function of the biological ion channels is to enhance the gating efficiency of the man-made systems. Herein, we demonstrate a DNA supersandwich and ATP gated nanofluidic device that exhibits high ON–OFF ratios (up to  $10^6$ ) and a perfect electric seal at its closed state ( $\sim G\Omega$ ). The ON–OFF ratio is distinctly higher than existing chemically modified nanofluidic gating systems. The gigaohm seal is comparable with that required in ion channel electrophysiological recording and some lipid bilayer-coated nanopore sensors. The gating function is implemented by self-assembling DNA supersandwich structures into solid-state nanochannels (open-to-closed) and their disassembly through ATP–DNA binding interactions (closed-to-open). On the basis of the reversible and all-or-none electrochemical switching properties, we further achieve the IMPLICATION logic operations within the nanofluidic structures. The present biohybrid nanofluidic device translates molecular events into electrical signals and indicates a built-in signal amplification mechanism for future nanofluidic biosensing and modular DNA computing on solid-state substrates.



## INTRODUCTION

Inspired by those genius designs in living organisms, such as the membrane ion channels and the nuclear pore complex, the development of artificial gatelike nanosystems able to perform programmed functions has elicited considerable interest and represents the forefront of the interdisciplinary fields of chemistry, materials science, and nanotechnology.<sup>1,2</sup> Typically in such systems, solid supports (e.g., solid-state nanopores, mesoporous nanoparticles, or electrochemical electrodes) are equipped with biological or synthetic molecules working as macromolecular actuators, transport receptors, or electronic transducers.<sup>3–9</sup>

Particularly, the specific Watson–Crick base pairing and programmable strand-displacement reactions make DNA an intriguing material for nanoscale science and engineering.<sup>10,11</sup> Many impressive achievements have been made in constructing DNA-based nanofluidic circuits and bioelectronic sensing devices in recent years.<sup>12–16</sup> Martin and co-workers fabricate a hairpin DNA functionalized nanotube membrane that selectively recognizes and transports the complementary strands with single-base resolution.<sup>17</sup> Ouyang and Jiang et al. build a compound DNA nanocompartment array on an electrode surface to investigate the nonequilibrium gating

mechanism of the flexible nanochannels formed by the compact DNA molecular motors.<sup>18</sup> We further integrate the stimulus-responsive DNA molecular motors with synthetic nanopores to construct pH and potassium gating, biohybrid nanofluidic devices, in which the ionic transport properties can be finely tuned by the proton and metal ion concentration.<sup>19,20</sup> Furthermore, these smart DNA-based nanofluidic systems find applications in bioinspired energy conversion and label-free detection of hazardous metal ions.<sup>21–24</sup> Early in this year, two groups of scientists reported independently a superior hybrid nanopore system by directly inserting DNA origami structures into solid-state nanopores.<sup>25,26</sup> This design strategy offer excellent adaptability, surface functionality, and biocompatibility that pave the way for future single-molecule nanopore sensors and the next-generation DNA sequencing.

Although substantial progress has been achieved in fabricating DNA and its analogues dressed switchable nanofluidic systems, challenges are still ahead of us.<sup>27–30</sup> For example, Rant and Dietz et al. point out that, even in the state-of-the-art DNA origami functionalized nanopore systems, the

Received: June 2, 2012

Published: September 6, 2012

DNA gatekeepers are permeable to small ions.<sup>26</sup> The leak ionic current and related current fluctuations would significantly reduce the resolution of the resistive-pulse sensing.<sup>31</sup> Therefore, an enhancement in gating efficiency of the DNA-nanopore hybrid system to ionic species is highly demanded.

In this article, we demonstrate a highly efficient and smart nanofluidic gating system that exhibits extremely high ON–OFF ratios (up to  $10^6$ ) and perfect electric seals at its closed state ( $\sim G\Omega$ ). The ON–OFF ratio is distinctly higher than that in existing chemically modified nanofluidic gating systems. The gigaohm seal is comparable with that required in ion channel electrophysiological recording and some lipid bilayer-coated nanopore sensors. Starting from the immobilized capture probe (CP) on the channel wall, the consecutive DNA hybridization creates long concatamers containing repeated units of probe 1 (P1) and probe 2 (P2) partially hybridized on different regions, which efficiently blocks the pathway for ion transport through the nanochannels (Figure 1). In addition, both the CP and P2

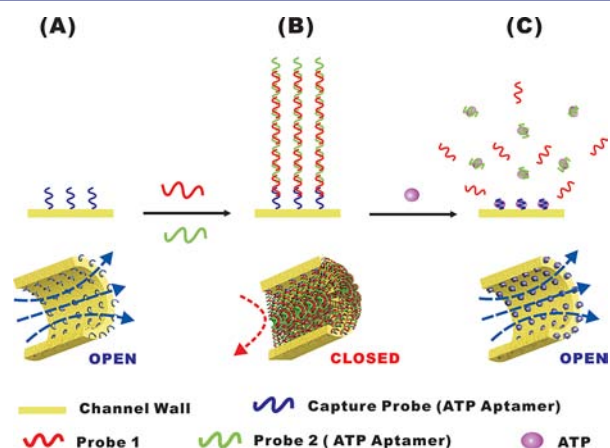


**Figure 1.** Gating of alumina nanochannels by DNA supersandwich assemblies and ATP. The nanochannels are first modified with the capture DNA probes (A). The DNA supersandwich structures initiate from the immobilized capture probes and compose repeated units of partially hybridized DNA probes 1 and 2 (B). The formed long DNA concatamers efficiently block the pathway for ion transport across the nanochannels, yielding an extremely low conducting state. Since the capture probe and probe 2 contain an ATP-binding sequence (CCTGGGGGATATGCGGAGGAAGG), the supersandwich structures are disassembled by ATP that reopens the conducting pathway (C).

are the DNA aptamers of ATP. After ATP treatment, disassembly of the supersandwich structures due to ATP–DNA binding interactions reopens the nanochannels. On the basis of the reversible and all-or-none electrochemical gating behavior, we further develop it into a DNA- and ATP-driven nanofluidic logic device performing the IMPLICATION operations.

## RESULTS AND DISCUSSION

Initially, the alumina nanochannels were chemically modified with the 5'-aminated capture DNA probes (35-mer) through a previously reported three-step process (Supporting Information (SI)).<sup>32</sup> After the addition of P1 and P2 in the environmental solution, concatenated supersandwich DNA structures containing multiple units of P1 and P2 grow from the CP on the channel wall. Gel electrophoresis is employed to evaluate the formation of the proposed supersandwich structures (Figure S1

in SI). The analysis shows a ladder of different lengths of the DNA concatamers with the maximum length being  $\sim 600$  base pairs. Mussi et al. show that, modified with short-chain oligonucleotides, the DNA assemblies attach on the periphery of the nanopore.<sup>33</sup> But in the present case, the length of the supersandwich DNA structure largely exceeds the radius of the nanochannel. Therefore, from the scanning electron microscopic (SEM) observation, one can see that the DNA assemblies densely pack on the membrane surface forming spherical nanoparticles (Figure 2B). The topography of the

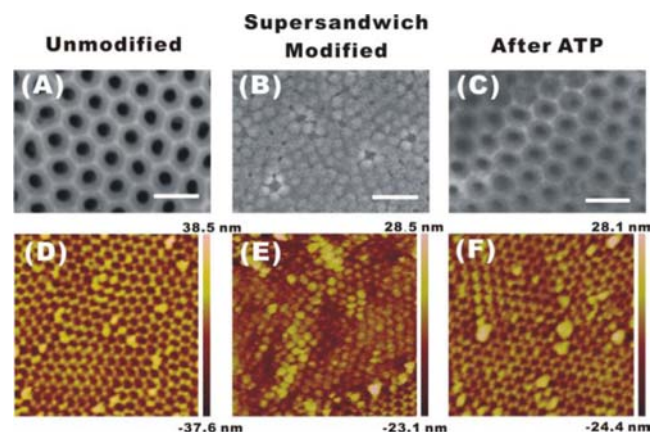


**Figure 2.** SEM (A–C) and AFM (D–F) characterizations of the DNA assembly and disassembly on the membrane surface. The mean pore diameter of the unmodified alumina nanochannels is  $56 \pm 3$  nm (A and D). After DNA assembly, spherical DNA nanoparticles densely pack on the membrane surface (B and E). After treatment with 1 mM ATP, most of the DNA nanostructures are removed from the membrane surface (C and F). The scale bar in SEM images is 200 nm. The scanning area in liquid-phase AFM is  $2 \mu\text{m} \times 2 \mu\text{m}$ .

DNA nanostructures on the membrane surface is further measured with atomic force microscopy (AFM) in liquid phase (Figure 2E and SI). The lateral size of the DNA nanoparticles is  $\sim 98$  nm, which perfectly covers the orifice of the nanochannels (Figure S5B in SI). Fortified by a laser scanning confocal microscopic (LSCM) measurement focused on the inner and outer membrane surface, we further prove that the DNA assembly also takes place inside the nanochannels (Figure 3). Another important feature of the specifically designed DNA supersandwich is that the CP and P2 are ATP aptamers. In the presence of ATP, the CP and P2 change their conformation to bind ATP, which consequently disassembles the supersandwich structures.<sup>34</sup> As proved by the SEM, AFM, and confocal fluorescent measurements, most of the DNA nanostructures in and out of the nanochannels are largely diminished after treatment with ATP (Figure 2C, F, and Figure 3C).

The significant change in surface topology and DNA loading properties caused by the autonomous assembly and ATP-driven disassembly of the DNA nanostructures leads to a highly efficient and smart nanofluidic gating system to the ionic species. After the modification with capture DNA, only very limited reduction in the transmembrane ionic current has been found (Figure S4 and Table S3 in SI). In contrast, after the DNA assembly, the ionic current sharply falls down from  $6.2 \times 10^{-5}$  A (the ON state) to  $1.1 \times 10^{-10}$  A (the OFF state) measured at +200 mV (Figure 4A). In addition, the ionic current recovers back to  $4.9 \times 10^{-5}$  A after being treated with 1 mM ATP. The ON–OFF ratio approaches  $10^5$ – $10^6$ . This

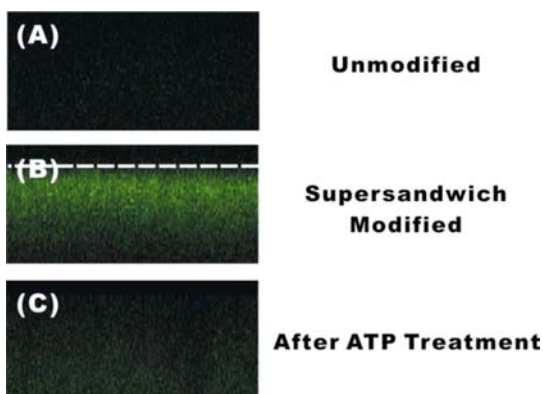


**Figure 3.** LSCM characterizations of the DNA assembly and disassembly inside the nanochannels. Strong fluorescent signal from the cross-sectional view of the membrane proves that the DNA assembly is also carried out inside the nanochannels (B). After being treated with ATP (1 mM), most of the DNA assemblies are removed from the nanochannels (C). The dashed line in (B) indicates the membrane surface. The fluorescent signals from (A) and (C) are so weak that the membrane surface cannot be identified from fluorescent images.

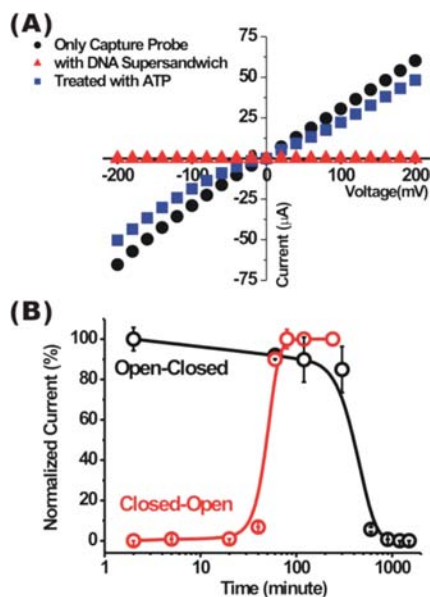


**Figure 4.** A switchable nanofluidic gating system manipulated by DNA supersandwich structure and ATP. (A) The distinct contrast in current–voltage responses of the functionalized nanochannels indicates a very high gating efficiency. The ON–OFF ratio approaches  $6 \times 10^5$ . After treatment with ATP (1 mM), the transmembrane current almost recovers back to its initial level. (B) Normalized current–time response of the smart nanochannels (measured at +200 mV) shows an asymmetric response time for about 500 (Open–Closed) and 100 min (Closed–Open). The mean channel width is about 60 nm.

performance is significantly improved than that of previously reported chemically modified nanofluidic gating systems, in which the ON–OFF ratios are typically less than 300-fold.<sup>35–38</sup> The highly effective blockade of the transmembrane ionic current stems from the greatly improved steric hindrance of the long DNA concatamers. In addition, the flexible nature of DNA is also a key factor for the highly improved gating efficiency. The microscopic flexibility makes DNA liable to fully plug the nanochannel,<sup>39</sup> compared with other “hard” nanoscale building

blocks, such as the metal nanoparticles<sup>40</sup> or the inorganic nanowires.<sup>41</sup> After being treated with ATP, the DNA supersandwich structures gradually disassemble due to the ATP binding to CP and P2. The dissociated DNA fragments can be easily washed away from the nanochannel, which reopens the conduction pathway.

For a switchable nanofluidic gating system, the response time is of great importance to evaluate the overall performance of the device. We have measured the time evolution of the transmembrane ionic current in both the Open–Closed and Closed–Open processes (Figure 4B). The ionic current was normalized to its fully opened state. The DNA supersandwich and ATP-gated nanochannels exhibit asymmetric response time for about 500 (Open–Closed) and 100 min (Closed–Open). The asymmetric response time has two implications. First, the response time discovered in the present nanofluidic system is much longer than that in bulk solution<sup>42,43</sup> and on the electrode surface.<sup>44</sup> This phenomenon mainly results from the steric constraint brought by the nanochannels.<sup>19,45</sup> Second, the assembly of DNA supersandwich structures inside nanochannels is slower than its inverse process. Besides the steric effect, the binding affinity between ATP and the target strands is stronger than that between partially hybridized DNA strands.<sup>46</sup> Thus, the melting of the DNA supersandwich structures is faster than the assembling process.

The switching properties are reproducible in a series of DNA functionalized nanochannels with different pore size ( $d$ ) ranging from 25 to 360 nm (Figure 5A). For comparison, we also test the gating properties in “traditional” DNA sandwich structure-functionalized nanochannels, in which each CP hybridized with merely one set of P1 and P2’ (modified sequences can be found in SI). For small nanochannels ( $d < 80$  nm), the ON–OFF ratios of the supersandwich structure-gated nanochannels are very high ( $>10^4$ ). The maximum ON–OFF ratios reach some  $10^5$ . Even in large nanochannels with orifices up to 360 nm, their gating efficiency still approaches  $10^2$ . In contrast, for the traditional DNA sandwich, considerable gating ratios can be found in smaller nanochannels, but they are more than 2 orders poorer than that of the DNA supersandwich structure-gated nanosystems. The molecular gating effects of the traditional DNA sandwich are almost invalid in large nanochannels ( $d > 250$  nm). Similar property has also been found in oligonucleotide modified nanopores.<sup>47,48</sup> That is because the relatively short DNA strands can not effectively block the ion conduction pathway through large channels. Therefore, the supersandwich DNA structures provide distinctly high gating efficiency in a wide range of channel widths.

Another important feature of the smart nanofluidic gating system is the nearly perfect electric seal at its closed state, which approaches  $\sim 1.2$  G $\Omega$  obtained with the optimized channel size of  $\sim 60$  nm (Figure 5B). Similarly, the OFF-state electric resistance for the supersandwich structure-functionalized nanochannels is about 2–3 orders higher than that for nanochannels modified with traditional sandwich structure. The gigaohm seal is comparable to the impedance between the glass micropipette and the cell membrane in ion channel electrophysiological recording,<sup>49</sup> and to that of the lipid bilayer-coated nanopore sensors.<sup>50,51</sup> The excellent electric seal makes it possible to reduce the background noise attributed to the unwanted leak current and provide a promising platform for reconstitution of biological or synthetic ion channels as hybrid nanopore sensors.

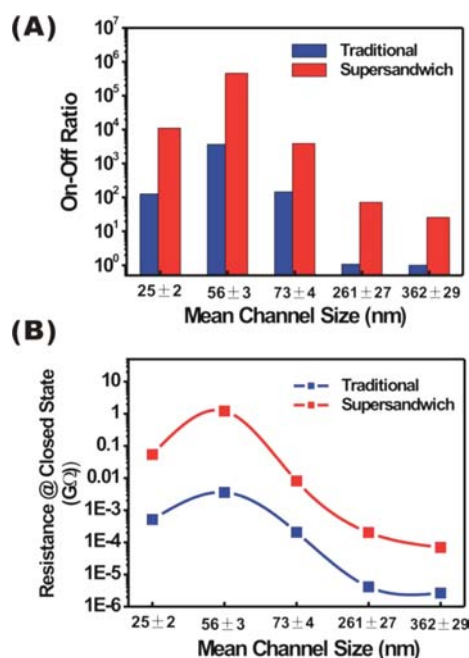


**Figure 5.** High gating efficiency and a nearly perfect electric seal can be realized in a series of nanochannels with different mean orifices ranging from 25 to 360 nm. (A) The supersandwich DNA structure works well in the whole range of channel sizes. The maximum ON–OFF ratios reach  $\sim 10^6$ . The traditional sandwich structure only works in the smaller nanochannels ( $d < 80$  nm), and it becomes invalid in larger nanochannels ( $d > 250$  nm). (B) The DNA supersandwich functionalized nanochannels exhibit ultrahigh electric resistance at its closed state. The maximum resistance achieves  $\sim 1.2$  G $\Omega$  with the optimized channel size of  $\sim 60$  nm. The membrane resistance for the supersandwich structure-modified nanochannels is about 2–3 orders higher than that of nanochannels modified with traditional sandwich structure.

The DNA concatamer-operated nanofluidic gating system is very reproducible. Parallel experiments on the alumina membranes with different pore size have been successfully repeated at least five times. Each time, we fabricated eight devices on one membrane (25 mm in diameter), generally half of which could properly work as a reversible nanofluidic device with high gating efficiency. In addition, the device can be reversibly switched between high- and low-conducting states at least in the first several cycles (Figure S9 in SI). In the following cycles, the devices show a remarkable decline in the gating efficiency. We propose that this phenomenon is associated with the instability of the DNA molecules and the 3-aminopropyl trimethoxysilane (APS) linker after the long time test of more than 30 h in aqueous solution (SI).<sup>52</sup> On the basis of our previous investigations on the reversible switching of DNA nanocontainers on electrode surface,<sup>45</sup> the reversibility of the nanofluidic switch, as well as the response time, might be further improved by, for example, modulating the ionic strength or adjusting the temperature.

The reversible and all-or-none nanofluidic gating system can be further developed into logic devices performing the IMPLICATION operation. The nanofluidic logic device employs ssDNA (P1 and P2, 1  $\mu$ M) and ATP (1 mM) as input signals and the change in transmembrane ionic current as output. For inputs, the presence of ssDNA or ATP in the environmental solution defines as “1” state, and the absence of these components defines as “0” state. For output, the signal

change of more than 100-fold (with respect to the state that only CP has been modified onto the nanochannels) defines as “1” states; otherwise, fewer increments or deductions in ionic current defines as “0” states.

We demonstrate the logic operations on eight parallel devices constructed on the same membrane. Before treatment with the molecular inputs, the  $I$ – $V$  behavior of the capture DNA-modified devices has been measured, respectively. From the current–voltage properties in response to the different combinations of input signals (Figure 6A), one can see that a distinct HIGH output (1) emerges if, and only if, both the ssDNA inputs are HIGH (1) and the ATP level is NONE (0). Otherwise, the output signals are all LOW (0). The changes in ionic conductance and the corresponding truth table are summarized in Figure 6B and C. Of note, the signal gain in “1” state is sufficiently high so that the different logic states can be easily distinguished. These features indicate that the biohybrid nanofluidic gating system functions as a high-contrast, three-input IMPLICATION logic device (Figure 6D).

In addition to the distinctly high conductance decrease in the (110) state, some minor conductance changes have been found in the (100) and (101) states. In the (100) case, only the probe 1 hybridizes to the capture DNA, resulting in a change in the effective pore size. A similar effect induced by DNA hybridization in nanopores has also been observed in previous reports by us and other groups.<sup>20,28</sup> In the (101) case, in the presence of ATP, the probe 1 can not hybridize onto the capture probe with embedded aptamer sequence for ATP (Table S1, SI).<sup>34</sup> The binding of ATP by capture DNA may alter the surface properties of the inner pore wall, which would consequently change the ion transport behavior of the nanopores.<sup>53</sup> Although the binding of ATP can be largely washed out with pure water,<sup>54</sup> minor changes to the signal can still be found.

To the best of our knowledge, it is the first time that IMPLICATION logic operations have been realized within nanofluidic systems. Although the IMPLICATION logic is seldom used in modern semiconductor-based computation and electrical engineering,<sup>55</sup> it is the foundation of the logical meaning of “necessity”.<sup>56,57</sup> More importantly, the integration of target binding properties of aptamers and the ever-proliferating DNA concatamers within nanofluidic structures translates molecular events into electrical signals and implements a built-in signal amplification mechanism for programmable sensing of nucleic acids and modular DNA computing on solid substrates.<sup>58–61</sup> In the future, the logic devices are expected to be concatenated together with the fluidic channels as communication medium to create multilevel computing circuits.<sup>62–64</sup>

## CONCLUSIONS

In conclusion, we have demonstrated a smart nanofluidic gating system with an extremely high ON–OFF ratio (up to  $\sim 10^6$ ) and a nearly perfect electric seal ( $\sim$ G $\Omega$ ) at its closed state. The gating function is implemented by self-assembly of DNA supersandwich structures into the nanochannels (the open-to-closed process) and their disassembly through ATP–DNA binding interactions (the closed-to-open process). The reversible and all-or-none switching properties make this biohybrid nanofluidic system a conceptually new set of nanofluidic logic devices performing the IMPLICATION operations. The present DNA- and ATP-gating nanosystem may have implications for future nanofluidic biosensing

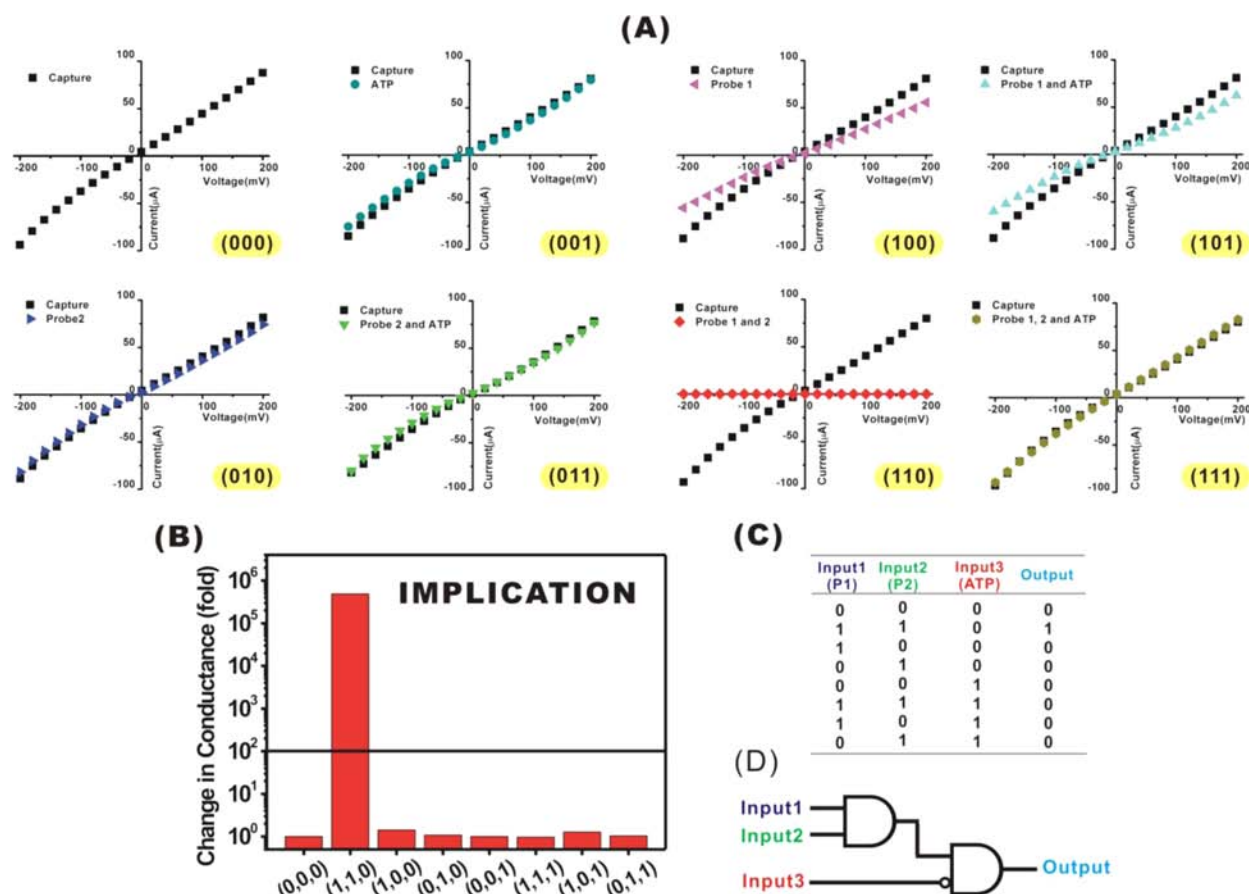


**Figure 6.** Operations of the three-input IMPLICATION nanofluidic logic device. P1, P2, and ATP are selected as inputs. The change in transmembrane ionic conductance is selected as output. From the current–voltage responses (A), we know that a distinct HIGH output (1) results if, and only if, both the ssDNA inputs are HIGH (1) and the ATP level is NONE (0). Otherwise, the output signals are all LOW (0). The corresponding truth table and symbolic expression are respectively shown in (C) and (D).

platforms with high signal-to-noise ratios and create an important paradigm for modular DNA computation on nanofluidic structures.

## EXPERIMENTAL SECTION

**Chemical Modification.** Cleaned alumina membranes containing straight nanochannels were first modified with 3-aminopropyl trimethoxysilane (APS) in acetone solution. After being thoroughly washed in acetone and baked at 120 °C for 2 h, the membranes were left in 25% aqueous solution of glutaraldehyde overnight. After that, the membranes were washed with distilled water and dried with argon gas. To immobilize the capture probe, the membranes were immersed in tris(hydroxymethyl)aminomethane hydrochloride solution (Tris-HCl, 10 mM, pH = 7.4, containing 500 mM NaCl, 1 mM  $\text{MgCl}_2$ ) with 5'-aminated capture DNA (1  $\mu\text{M}$ ) for 10 h. For DNA hybridization, the membranes were rinsed with distilled water and put into Tris solution containing P1 and P2 (1  $\mu\text{M}$ ) for 18 h. For ATP dehybridization, the membranes were immersed in Tris solution containing 1 mM ATP for two hours, and then thoroughly washed with Tris solution before electrical measurements. Experimental details can be found in SI. The DNA sequences used in this work were: CP, 5'-NH<sub>2</sub>-(CH<sub>2</sub>)<sub>6</sub>-CGGCACCTGGGGGAGTATTGCG-GAGGAAGGTGCCG-3'; P1, 5'-TACTCCCCAGGT-GCCGACGGCACCTTCCTCCGCA-3'; P2, 5'-CGGCACCTGGGGGAGTATTGCGGAGGAAGGTGCCG-3'; P2', 5'-CGGCACCTGGGGGAGTGAT-3' (for traditional sandwich structure).

**Characterization of the DNA Assemblies.** The DNA nanostructures on the membrane surface were characterized by SEM

(Hitachi S-4800) observation (without metal coating) and contact-mode AFM (Veeco MultiMode 8) measurement in liquid phase. To confirm that the DNA assembly also took place inside the nanochannel, a fluorescein isothiocyanate (FITC) labeled P2 on the 3'-end was used. The fluorescent signal was imaged by a laser scanning confocal microscope (Olympus FV1000). The laser penetration depth is  $\sim 30 \mu\text{m}$ .

**Electrical Measurements.** A piece of nanochannel membrane was mounted in between a two-compartment electrochemical cell as described in our previous work.<sup>65</sup> The transmembrane ionic current was measured with a Keithley 6487 picoammeter/voltage source (Keithley Instruments) through Ag/AgCl electrodes. The total size of a membrane device is about 40 mm<sup>2</sup>. The effective area for ionic conduction measurements was  $\sim 0.7 \text{ mm}^2$ . The electrolyte was 100 mM KCl solution (pH  $\sim 5.8$ ).

## ASSOCIATED CONTENT

### Supporting Information

(1) Materials and methods; (2) characterization of the pristine nanoporous membrane; (3) chemical modification of the nanoporous membrane; (4) DNA supersandwich structures on the membrane surface; (5) current–voltage measurements of traditional and supersandwich structures modified nanochannels; (6) the reversibility of the DNA actuated nanofluidic gating device. This material is available free of charge via the Internet at <http://pubs.acs.org>.

## ■ AUTHOR INFORMATION

## Corresponding Author

wguo@iccas.ac.cn (W.G.); xiafan@mail.hust.edu.cn (F.X.)

## Author Contributions

<sup>†</sup>These authors contributed equally.

## Notes

The authors declare no competing financial interest.

## ■ ACKNOWLEDGMENTS

We thank Prof. Dong Han (NCNST) and Dr. Bin Su (ICCAS) for beneficial discussions. Gel electrophoresis tests are kindly provided by Prof. Dongsheng Liu and Prof. Jinghong Li in Tsinghua University (Beijing). This work is financially supported by the National Research Fund for Fundamental Key Projects (2012CB933200, 2011CB935700, 2010CB934700, 2009CB930404) and the National Natural Science Foundation of China (90923004, 91127025, 20920102036, 20974113, 21071148, 21121001, 21103201). The Chinese Academy of Sciences is gratefully acknowledged.

## ■ REFERENCES

- (1) Hou, X.; Guo, W.; Jiang, L. *Chem. Soc. Rev.* **2011**, *40*, 2385.
- (2) Sparreboom, W.; van den Berg, A.; Eijkel, J. C. T. *Nat. Nanotechnol.* **2009**, *4*, 713.
- (3) Gyurcsanyi, R. E. *TrAC, Trends Anal. Chem.* **2008**, *27*, 627.
- (4) Casasus, R.; Climent, E.; Marcos, M. D.; Martinez-Manez, R.; Sancenon, F.; Soto, J.; Amoros, P.; Cano, J.; Ruiz, E. *J. Am. Chem. Soc.* **2008**, *130*, 1903.
- (5) Ali, M.; Mafe, S.; Ramirez, P.; Neumann, R.; Ensinger, W. *Langmuir* **2009**, *25*, 11993.
- (6) Cauda, V.; Engelke, H.; Sauer, A.; Arcizet, D.; Brauchle, C.; Radler, J.; Bein, T. *Nano Lett.* **2010**, *10*, 2484.
- (7) Zhu, C. L.; Lu, C. H.; Song, X. Y.; Yang, H. H.; Wang, X. R. *J. Am. Chem. Soc.* **2011**, *133*, 1278.
- (8) Yang, Y.; Liu, G.; Liu, H. J.; Li, D.; Fan, C. H.; Liu, D. S. *Nano Lett.* **2010**, *10*, 1393.
- (9) Zhou, Y.; Guo, W.; Cheng, J.; Liu, Y.; Li, J.; Jiang, L. *Adv. Mater.* **2012**, *24*, 962.
- (10) Wilner, O. I.; Willner, I. *Chem. Rev.* **2012**, *112*, 2528.
- (11) Zhang, D. Y.; Seelig, G. *Nature Chem.* **2011**, *3*, 103.
- (12) Harrell, C. C.; Kohli, P.; Siwy, Z.; Martin, C. R. *J. Am. Chem. Soc.* **2004**, *126*, 15646.
- (13) Ali, M.; Neumann, R.; Ensinger, W. *ACS Nano* **2010**, *4*, 7267.
- (14) Venkatesan, B. M.; Bashir, R. *Nat. Nanotechnol.* **2011**, *6*, 615.
- (15) Ying, Y. L.; Wang, H. Y.; Sutherland, T. C.; Long, Y. T. *Small* **2011**, *7*, 87.
- (16) Pennisi, E. *Science* **2012**, *336*, 534.
- (17) Kohli, P.; Harrell, C. C.; Cao, Z.; Gasparac, R.; Tan, W.; Martin, C. R. *Science* **2004**, *305*, 984.
- (18) Mao, Y.; Chang, S.; Yang, S.; Ouyang, Q.; Jiang, L. *Nat. Nanotechnol.* **2007**, *2*, 366.
- (19) Xia, F.; Guo, W.; Mao, Y. D.; Hou, X.; Xue, J. M.; Xia, H. W.; Wang, L.; Song, Y. L.; Ji, H.; Qi, O. Y.; Wang, Y. G.; Jiang, L. *J. Am. Chem. Soc.* **2008**, *130*, 8345.
- (20) Hou, X.; Guo, W.; Xia, F.; Nie, F. Q.; Dong, H.; Tian, Y.; Wen, L. P.; Wang, L.; Cao, L. X.; Yang, Y.; Xue, J. M.; Song, Y. L.; Wang, Y. G.; Liu, D. S.; Jiang, L. *J. Am. Chem. Soc.* **2009**, *131*, 7800.
- (21) Guo, W.; Cao, L. X.; Xia, J. C.; Nie, F. Q.; Ma, W.; Xue, J. M.; Song, Y. L.; Zhu, D. B.; Wang, Y. G.; Jiang, L. *Adv. Funct. Mater.* **2010**, *20*, 1339.
- (22) Cao, L.; Guo, W.; Ma, W.; Wang, L.; Xia, F.; Wang, S.; Wang, Y.; Jiang, L.; Zhu, D. *Energy Environ. Sci.* **2011**, *4*, 2259.
- (23) Wen, L. P.; Hou, X.; Tian, Y.; Zhai, J.; Jiang, L. *Adv. Funct. Mater.* **2010**, *20*, 2636.
- (24) Wen, S.; Zeng, T.; Liu, L.; Zhao, K.; Zhao, Y.; Liu, X.; Wu, H.-C. *J. Am. Chem. Soc.* **2011**, *133*, 18312.
- (25) Bell, N. A. W.; Engst, C. R.; Ablay, M.; Divitini, G.; Ducati, C.; Liedl, T.; Keyser, U. F. *Nano Lett.* **2012**, *12*, 512.
- (26) Wei, R.; Martin, T. G.; Rant, U.; Dietz, H. *Angew. Chem., Int. Ed.* **2012**, *51*, 4864.
- (27) Dekker, C. *Nat. Nanotechnol.* **2007**, *2*, 209.
- (28) Iqbal, S. M.; Akin, D.; Bashir, R. *Nat. Nanotechnol.* **2007**, *2*, 243.
- (29) Li, S. J.; Li, J.; Wang, K.; Wang, C.; Xu, J. J.; Chen, H. Y.; Xia, X. H.; Huo, Q. *ACS Nano* **2010**, *4*, 6417.
- (30) Garaj, S.; Hubbard, W.; Reina, A.; Kong, J.; Branton, D.; Golovchenko, J. A. *Nature* **2010**, *467*, 190.
- (31) Hall, A. R.; Scott, A.; Rotem, D.; Mehta, K. K.; Bayley, H.; Dekker, C. *Nat. Nanotechnol.* **2010**, *5*, 874.
- (32) Vlasiouk, I.; Krasnoslobodtsev, A.; Smirnov, S.; Germann, M. *Langmuir* **2004**, *20*, 9913.
- (33) Mussi, V.; Fanzio, P.; Repetto, L.; Firpo, G.; Stigliani, S.; Tonini, G. P.; Valbusa, U. *Biosens. Bioelectron.* **2011**, *29*, 125.
- (34) Huizenga, D. E.; Szostak, J. W. *Biochemistry* **1995**, *34*, 656.
- (35) Jagerszki, G.; Gyurcsanyi, R. E.; Hofler, L.; Pretsch, E. *Nano Lett.* **2007**, *7*, 1609.
- (36) Schepelina, O.; Zharov, I. *Langmuir* **2007**, *23*, 12704.
- (37) Abelov, A. E.; Schepelina, O.; White, R. J.; Vallee-Belisle, A.; Plaxco, K. W.; Zharov, I. *Chem. Commun.* **2010**, *46*, 7984.
- (38) Guo, W.; Xia, H.; Cao, L.; Xia, F.; Wang, S.; Zhang, G.; Song, Y.; Wang, Y.; Jiang, L.; Zhu, D. *Adv. Funct. Mater.* **2010**, *20*, 3561.
- (39) Fan, R.; Karnik, R.; Yue, M.; Li, D.; Majumdar, A.; Yang, P. *Nano Lett.* **2005**, *5*, 1633.
- (40) Zhu, B.; Li, J. J.; Chen, Q. W.; Cao, R. G.; Li, J. M.; Xu, D. S. *Phys. Chem. Chem. Phys.* **2010**, *12*, 9989.
- (41) Goldberger, J.; Fan, R.; Yang, P. *Acc. Chem. Res.* **2006**, *39*, 239.
- (42) Li, T.; Wang, E. K.; Dong, S. J. *J. Am. Chem. Soc.* **2009**, *131*, 15082.
- (43) Wang, F.; Elbaz, J.; Orbach, R.; Magen, N.; Willner, I. *J. Am. Chem. Soc.* **2011**, *133*, 17149.
- (44) Xia, F.; White, R. J.; Zuo, X. L.; Patterson, A.; Xiao, Y.; Kang, D.; Gong, X.; Plaxco, K. W.; Heeger, A. J. *J. Am. Chem. Soc.* **2010**, *132*, 14346.
- (45) Mao, Y.; Liu, D.; Wang, S.; Luo, S.; Wang, W.; Yang, Y.; Ouyang, Q.; Jiang, L. *Nucleic Acids Res.* **2007**, *35*, e33.
- (46) Tang, Z. W.; Mallikaratchy, P.; Yang, R. H.; Kim, Y. M.; Zhu, Z.; Wang, H.; Tan, W. H. *J. Am. Chem. Soc.* **2008**, *130*, 11268.
- (47) Vlasiouk, I.; Takmakov, P.; Smirnov, S. *Langmuir* **2005**, *21*, 4776.
- (48) Wang, X.; Smirnov, S. *ACS Nano* **2009**, *3*, 1004.
- (49) Hille, B. *Ion Channels of Excitable Membranes*; Sinauer Associates Inc.: Sunderland, MA, 2001.
- (50) White, R. J.; Ervin, E. N.; Yang, T.; Chen, X.; Daniel, S.; Cremer, P. S.; White, H. S. *J. Am. Chem. Soc.* **2007**, *129*, 11766.
- (51) Venkatesan, B. M.; Polans, J.; Comer, J.; Sridhar, S.; Wendell, D.; Aksimentiev, A.; Bashir, R. *Biomed. Microdevices* **2011**, *13*, 671.
- (52) Szczepanski, V.; Vlasiouk, I.; Smirnov, S. *J. Membr. Sci.* **2006**, *281*, 587.
- (53) Ali, M.; Nguyen, Q. H.; Neumann, R.; Ensinger, W. *Chem. Commun.* **2010**, *46*, 6690.
- (54) Zuo, X.; Xiao, Y.; Plaxco, K. W. *J. Am. Chem. Soc.* **2009**, *131*, 6944.
- (55) Borghetti, J.; Snider, G. S.; Kuekes, P. J.; Yang, J. J.; Stewart, D. R.; Williams, R. S. *Nature* **2010**, *464*, 873.
- (56) Russell, B. *The Principles of Mathematics*; Cambridge University Press: Cambridge, 1903.
- (57) Pelham, J. *Topoi* **1999**, *18*, 175.
- (58) Willner, I.; Zayats, M. *Angew. Chem., Int. Ed.* **2007**, *46*, 6408.
- (59) Frezza, B. M.; Cockroft, S. L.; Ghadiri, M. R. *J. Am. Chem. Soc.* **2007**, *129*, 14875.
- (60) Xia, F.; Zuo, X. L.; Yang, R. Q.; White, R. J.; Xiao, Y.; Kang, D.; Gong, X. O.; Lubin, A. A.; Vallee-Belisle, A.; Yuen, J. D.; Hsu, B. Y. B.; Plaxco, K. W. *J. Am. Chem. Soc.* **2010**, *132*, 8557.
- (61) de Ruiter, G.; van der Boom, M. E. *Acc. Chem. Res.* **2011**, *44*, 563.

- (62) Gupta, T.; van der Boom, M. E. *Angew. Chem., Int. Ed.* **2008**, *47*, 5322.
- (63) Mafe, S.; Manzanares, J. A.; Ramirez, P. J. *Phys. Chem. C* **2010**, *114*, 21287.
- (64) Guliyev, R.; Ozturk, S.; Kostereli, Z.; Akkaya, E. U. *Angew. Chem., Int. Ed.* **2011**, *50*, 9826.
- (65) Guo, W.; Xia, H.; Xia, F.; Hou, X.; Cao, L.; Wang, L.; Xue, J.; Zhang, G.; Song, Y.; Zhu, D.; Wang, Y.; Jiang, L. *ChemPhysChem* **2010**, *11*, 859.